

RSC Advances



This is an *Accepted Manuscript*, which has been through the Royal Society of Chemistry peer review process and has been accepted for publication.

Accepted Manuscripts are published online shortly after acceptance, before technical editing, formatting and proof reading. Using this free service, authors can make their results available to the community, in citable form, before we publish the edited article. This *Accepted Manuscript* will be replaced by the edited, formatted and paginated article as soon as this is available.

You can find more information about *Accepted Manuscripts* in the [Information for Authors](#).

Please note that technical editing may introduce minor changes to the text and/or graphics, which may alter content. The journal's standard [Terms & Conditions](#) and the [Ethical guidelines](#) still apply. In no event shall the Royal Society of Chemistry be held responsible for any errors or omissions in this *Accepted Manuscript* or any consequences arising from the use of any information it contains.

Insights into the adsorption of simple benzene derivatives on carbon nanotubes

Yonglan Liu,^a Jin Zhang,^a Xiaohua Chen,^b Jie Zheng,^c Guixue Wang,^a and Guizhao Liang^{*a}

5

^a Key Laboratory of Biorheological Science and Technology
Ministry of Education, School of Bioengineering
Chongqing University, Chongqing 400044, China, E-mail: gzliang@cqu.edu.cn

10

^b School of Chemistry and Chemical Engineering, Chongqing University, Chongqing, 400044,
P. R. China

15

^c Department of Chemical and Biomolecular Engineering
The University of Akron, Akron, Ohio 44325, USA

20 Electronic Supplementary Information (ESI) available:

Figure S1 displays two types of π - π packing; Figure S2 displays the bridge configuration of the benzene-SWCN system; Figure S3 displays the difference of surface characteristics, dipole moments and orbital energies between benzene and its derivatives; Figure S4 indicates the dihedral angle formed by 4 atoms in chlorobenzene; Figure S5 displays the difference of dipole moments between SWCNs and X-IntSWCNs; Figure S6 displays the difference of various energies between SWCNs and X-IntSWCNs; Figure S7 displays the final optimized configurations of 25 molecule-SWCN systems in water; Text S1 summarizes the electronegativity(substituent)-adsorption relationships; Table S1 lists Cook's distance and leverage values of 25 simple molecules; Table S2 lists substituents and dihedral angles (Φ) of 25 simple molecules; Table S3 contains various predicted energies (kcal/mol) for 25 molecule-SWCN systems in the gas phase; Table S4 contains various predicted energies (kcal/mol) for 25 molecule-SWCN systems in water; Table S5 lists the Cartesian coordinates for 25 molecule-SWCN systems in the gas phase and water calculated at the M062X/6-31G(d) levels of theory.

35

40

To explore the adsorption characteristics of small molecules on carbon nanotubes (CNs) is important for rational design of CN-based materials for many applications. In this work, we construct a quantitative structure-activity relationship (QSAR) model to predict the adsorption of 25 simple benzene derivatives on CNs, and investigate the molecule-SWCN interactions by density functional theory (DFT) calculations, with the M062X functional at the 6-31G(d) basis set. The QSAR model exhibits a regression correlation coefficient (R_{rm}^2) of 0.986 and a cross-validated coefficient (Q_{cv}^2) of 0.968. A total of more than 200 optimizations are carried out to determine preferential interaction modes, binding conformations, and underlying driving forces of the molecule-SWCN systems. We show the bridge configuration is the preferred molecule-SWCN interaction mode, which is mainly governed by π - π stacking; the molecules have experienced a significant electron rearrangement whereas the SWCNs have a weak one due to the molecule-SWCN mutual forces; and the substituents play dual effects on the adsorption by two ways, i.e., indirectly affecting π - π stacking by altering the electron density of the benzene ring and directly interacting with the nanotube surface. This work provides insights into noncovalent functionalization of CNs, and adsorption and desorption of simple organic molecules on CNs.

20

25

30

35

40

1. Introduction

Carbon nanotubes (CNs) including single-walled and multiple-walled CNs (SWCNs and MWCNs) have continuously attracted considerable attentions since the first discovery in 1976.¹ Their unique functional, mechanical, electrical, and optoelectronic properties outperform classical materials of organic polymers and semiconductors² in a broad range of fundamental and practical applications, including electronic devices,² nanowires³, quantum computers,⁴ and drug delivery carriers and diagnostic devices.^{5, 6} High-performance of CN-based materials heavily relies on their synergistic interactions with many different host materials. Such synergistic interactions often involve different noncovalent forces and complex interplay among CNs, host materials, environmental molecules, and other involved molecules of interest.

Study on the interactions of small molecules with CNs is critical for (i) indirectly mapping the characteristics of the ‘nano-bio’ interface,⁵ (ii) fundamentally understanding how CNs effectively adsorb toxic organic chemicals from their surrounding environments,^{6, 7} and (iii) providing insights into functional CNs with specific properties.⁸⁻¹¹ Significant efforts and great progress have been made to study molecule-CN systems.¹²⁻¹⁵ However, how molecules and CNs interact with each other is still poorly understood due to complex interplay among small molecules, CNs, and environments.¹⁴

Computational approaches are often used to investigate actions of CNs with various small molecules, thereby to assess potential risk and new functions for the CNs conjugated with small molecules.¹⁵⁻¹⁸ The quantitative structure-activity relationship (QSAR) is one of powerful computational methods for rational design of drugs, materials, catalysts, and proteins/peptides with desirable activities and functions.¹⁹⁻²⁵ Particularly, QSAR models have been utilized in many nano-science fields²² for prediction of biological activity²⁶ and cytotoxicity of nanoparticles,²³ study on adsorption mechanisms of aromatic contaminants by MWCNs,¹⁸ and characterization of surface adsorption forces of nanomaterials.^{27, 28} The weak interactions between the molecular π orbitals and the extended π Bloch states of the nanotubes are characterized by the dispersive forces that lead to stacking in flat configurations of the molecules on the pristine sidewalls¹⁵⁻¹⁷ and which can be altered by the presence of substitutional groups in the molecule.^{29, 30} Accurate theoretical descriptions of weak interactions could be acquired by density function theory (DFT) calculations.¹⁵⁻¹⁷

Simple benzene derivatives have been often used as probe compounds to characterize or modify the properties of nanomaterials²⁸ and biological activities.^{31, 32} They are also generally regarded as arch-criminals in environmental pollution.³³ In this work, we employed QSAR modeling and DFT simulations to explore the structure-dynamics-adsorption relationship of simple benzene derivatives with SWCNs. A QSAR model was constructed to predict the molecule-SWCN adsorption. Various interaction modes were designed to illustrate the preferential molecule-SWCN conformations. DFT calculations were further used to optimize the structural, dynamic, and energetic aspects of the molecule-SWCN complexes and to determine underlying adsorption mechanisms. We also investigated how molecules and SWCNs mutually affected their properties. This work provides helpful information about the interaction formations, affinities, and modes between small molecules and SWCNs which is beneficial to understanding nanotoxicity and nanobiology.

2. Principles and methods

2.1 Experimental adsorptions

Structures and adsorption activities of training set including 25 simple benzene derivatives were collected from Xia's work²⁸ (Table 1). These molecules have been widely used as probe compounds for predicting biological activities.^{28, 31, 34} The adsorption coefficients (k) were obtained by measuring the quantities of the compounds adsorbed on the surfaces of the MWCNs and the equilibrium concentrations of the compounds in the media. The log k values, as dependent variables, were applied to build the QSAR model.

2.2 Nano-descriptor calculations

Three-dimensional structures of 25 molecules were constructed by Sybyl 8.1 (<http://www.certara.com/>), followed by the structural optimization with DFT calculations based on the M062X³⁵ functional at the 6-31G(d) basis set. Vibrational frequencies were further computed at the same level to ensure no imaginary frequency for the optimized structures. Then, 79 three-dimensional structural parameters, i.e., Surface area, Volume and Shape (SurVolSha) descriptors, were computed to characterize the structural characteristics of the 25 molecules.

2.3 QSAR modeling and validation

Multiple linear regression (MLR) was used to generate the QSAR model. The SurVolSha descriptors as inputs of the MLR model were selected by a stepwise method³⁶ to delete redundant descriptors, thereby to make the model more interpretable. The selection of the variables was based on F value of partial F test (The variable was accepted by the model if the F value was larger than 3.84, otherwise rejected if the F value was less than 2.71). A leave-one-out (LOO)³⁷ cross-validation was employed to test the predictive ability of the model. The modeling performance was assessed based on a serial of statistical parameters, including multiple correlation coefficients, standard error and Fisher's criterion, etc.

2.4 Molecule-SWCN interaction optimization

To reduce the computational complexity, we used SWCNs, instead of MWCNs, to probe the molecule-SWCN interaction modes. We built an armchair SWCN (3, 3) with a diameter of 4.07 Å, a length of 12.30 Å along the tube axis, and added terminating hydrogen atoms to both ends of the SWCNs using Materials Studio (<http://accelrys.com/products/materials-studio/>). A total of 6 to 10 interaction modes were designed to explore the potential interaction configuration for each molecule-SWCN system in the gas phase. All geometries were completely optimized in all internal degrees of freedom using DFT at the M062X/6-31G(d) levels of theory. For all the optimized models, frequency calculations were subsequently performed, with no imaginary frequency results. As a result, the global minimum points were recognized, and the ultimate conformation and a serial of quantum-chemical parameters, including various energies, surface characteristics, dipole moments, etc., were obtained.

Interaction energy (ΔE_{Int}) and adsorption energy (ΔE_{Ads}) are defined as follows:

$$\Delta E_{\text{Int}} = E_{\text{Mol-SWCN}}^{\text{Mol-SWCN}} - E_{\text{Mol-SWCN}}^{\text{SWCN}} - E_{\text{Mol-SWCN}}^{\text{Mol}} \quad (1)$$

$$\Delta E_{\text{Ads}} = E_{\text{Mol-SWCN}}^{\text{Mol-SWCN}} - E_{\text{SWCN}}^{\text{SWCN}} - E_{\text{Mol}}^{\text{Mol}} \quad (2)$$

Where ΔE_{Ads} stands for the energy difference between the complex and infinitely separated fragments (Molecule and SWCN), and ΔE_{Int} corresponds to the fragments with the geometry of the complex.³⁸

The difference between adsorption energy and interaction energy is termed as the deformation energy, E_{Def} , of the fragments, that is:

$$\Delta E_{\text{Ads}} = \Delta E_{\text{Int}} + E_{\text{Def}}^{\text{SWCN}} + E_{\text{Def}}^{\text{Mol}} \quad (3)$$

$$E_{\text{Def}}^{\text{SWCN}} = E_{\text{Mol-SWCN}}^{\text{SWCN}} - E_{\text{SWCN}}^{\text{SWCN}} \quad (4)$$

$$E_{\text{Def}}^{\text{Mol}} = E_{\text{Mol-SWCN}}^{\text{Mol}} - E_{\text{Mol}}^{\text{Mol}} \quad (5)$$

To elucidate solvent effects on the adsorption of the molecules with the SWCNs, based on the most stable gas-phase modes, we comparably computed the characteristic parameters of the complexes and fragments in water by an integral equation formalism polarized continuum model IEF-PCM method.³⁹ All DFT and IEF-PCM calculations were performed using Gaussian 09⁴⁰ on a 256-processor Shuguang server. In what follows, for convenience, we employed the abbreviations, X-Mol, X-IntMol, and X-IntSWCN, to indicate the optimized single molecules, the molecules and the SWCNs derived from the optimized molecule-SWCN systems, respectively. (Here, X is the number of molecules or SWCNs).

3. Results and discussion

This work mainly aims to address two critical questions for fundamentally understanding the molecule-SWCN interactions: to construct a predictive model for assessing the adsorption of the benzene derivatives on the SWCNs, and to explore the binding modes of the derivatives with the SWCNs. Difficulty and complexity from complicated experimental procedures, accompanying with an expansion of small molecules in public databases, have challenged and motivated development of high-throughput computational methods for prediction and determination of their adsorptions and interactions with the SWCNs. Accordingly, to address the issues above, we employed a combination of QSAR modeling and DFT calculations to illustrate the binding characteristics of the benzene derivatives with the SWCNs.

3.1 Predictive capability of the QSAR model

Through the stepwise method, we selected 8 variables (Table 2) from 79 SurVolSha descriptors, which characterized the structural connectivity and conformation of the 25 molecules, and adopted them to generate the MLR-based QSAR model. Multiple correlation coefficient, standard deviation, and Fisher test value of regression modeling were $R_{\text{rm}}^2=0.986$, $SE_{\text{rm}}=0.109$, and $F_{\text{rm}}=137.920$, respectively, indicating the model can robustly correlate the 8 SurVolSha variables and experimental adsorption coefficients. As displayed in Table 2, the magnitude of multicollinearity is relatively low according to a cut off value (10.000) of variance inflation factors of each variable.⁴¹ Furthermore, the *t*-test absolute value of each variable is larger than 2.000, suggesting each variable has a significant impact on dependent *Y* values (adsorption coefficients). Besides, Cook's distance and leverage values (Table S1) further confirm that excluding an observation from computation of the regression statistics weakly changes the coefficients. With the LOO cross-validation, multiple correlation coefficient (Q_{cv}^2) of 0.968 was greater than 0.700, as a demonstration of the predictive robustness of the QSAR model.⁴²

We evaluated the relative importance of the 8 SurVolSha variables based on partial correlation coefficients of the model. Table 2 shows that surface rugosity, a measure of small-scale variations or amplitude at the height of a surface (real surface area/geometric surface area), possesses a largest positive partial coefficient (0.937), indicating this variable makes a relatively largest positive contribution to adsorption coefficients. The second largest positive contributor to adsorption coefficients is the capacity factor variable (0.855), which represents the ratio of the hydrophilic surface over the total molecular surface; in other words, it is the hydrophilic surface per surface unit.⁴³ The only variable H-bond donor capacity has a negative coefficient (-0.928), meaning a stronger H-bond donor capacity can make a smaller contribution to adsorption coefficients.

3.2 π - π stacking as a dominant adsorption factor

As we know, the SWCNs have multiple π orbital perpendicular to their surface,¹⁷ while the benzene derivatives studied here have at least one π structure from the aromatic ring. Hence, the benzene derivatives with different substituents are expected to have different interaction modes with the SWCNs. As a proof-of-concept, we designed 8 representative chlorobenzene-SWCN modes to account for the most possible interaction manners (Fig. 1). The parallel modes, involving the hollow, umbrella, bridge and cross manners, mainly correspond to the configurational effects of benzene rings on their preferential adsorptions on the SWCNs, while the perpendicular modes, involving R-pointing, para-R-pointing, parallel and perpendicular side-lying manners, mainly correspond to the effects of the substituents on the molecule-SWCN interactions. Finally, a total of 187 interaction modes were designed to examine possible molecule-SWCN interaction configurations.

The final optimized molecule-SWCN configurations (Fig. 2) display the parallel modes have higher occurrence probabilities than the perpendicular modes, indicating the parallel modes are more stable than the perpendicular modes for the same molecule-SWCN system; moreover, the face-to-face π - π packing other than the face-to-side packing (Fig. S1) dominates the adsorption interaction of the aromatic molecules on the SWCNs. Through a systematic comparison, we show that the approximate bridge configuration is the most favorable molecule-SWCN interaction mode, in agreement with the conclusion on the interaction configuration of benzene or its several simple derivatives with the SWCNs.^{15, 17}

Five types of interactions, including π - π stacking, hydrophobic effects, hydrogen bonds, and electrostatic and covalent interactions, have been recognized as major driving forces for the adsorption of organic chemicals on carbon nanosized particle surface,^{33, 44} but their relative contributions are difficult to be quantified.⁴⁵ Here, we depicted the isosurfaces to qualitatively represent the weak interactions between the molecules and the SWCNs based on reduced-density gradient (RDG) analysis,⁴⁶ where RDG was defined as $RDG(r)=|\nabla\rho(r)|/\rho^{4/3}(r)$ with ρ =electron density of the whole system. The interaction visualizations of 25 molecule-SWCN systems clearly show two general interaction regions of phenyl-surface and substituent-surface between the molecules and the SWCNs (Fig. 3). Relative sizes of two regions suggest the π - π interaction between the benzene ring and the SWCN surface is a dominant adsorption factor.^{17, 47}

The benzene-SWCN simulation (Fig. S2) brings out an interaction energy of -6.886 kcal/mol for benzene on the SWCN, which occupies ~64.83% of the average interaction

energy (-10.621 kcal/mol) for the 25 benzene derivatives on the SWCNs, further demonstrating π - π packing plays a main role in the adsorption process.

The third evidence for the dominant adsorption role of π - π stacking is that 3 molecules with double benzene rings (naphthalene, 1-methylnaphthalene and biphenyl) have 3 top adsorption values in all the compounds studied, and the average adsorption value (4.837) of these 3 molecules is larger than that of (3.417) the other 22 molecules only with a single benzene ring. This illustrated the contribution of the substituent to the adsorption is generally less than that of π - π packing, thus double π - π packing have larger effects on the adsorption than a combination of single π - π packing and substituent(s).

We do not consider the adsorption mechanisms of small molecules on various CNTs with different sizes (diameter and length), but mainly focus on the adsorption characteristics of 25 benzene derivatives containing different functional groups on SWCNs other than MWCNs, thereby to explore some common adsorption rules of these molecules with SWCNs. This is because on the one hand, a large CNT system will require high computational power; on the other hand, the interaction mechanism between small benzene derivatives and CNTs do not depend on the size of CNTs, which has been confirmed by the report¹⁵ that the noncovalent π - π interaction between the benzene ring and the CNTs with various diameters and chiral angles is the dominant adsorption mechanism. Our results have shown the adsorption mechanism of small benzene derivatives with SWCNs mainly relies on the noncovalent π - π interaction between the benzene ring and the tube regardless of the charge-transfer properties of the functional groups or the orientations of small molecules toward the tube surface.

3.3 Effects of substituents on the molecule-SWCN adsorptions

As the analysis mentioned above, the π - π interaction is significant in the adsorption process, but is not the only factor. This is because, on the one hand, π - π stacking could not account for the remaining ~35.17% of the average molecule-SWCN interaction energies (-10.621 kcal/mol); on the other hand, surface characteristics (van der Waals volume, positive surface area, and negative surface area) and various orbital energies of the 25 small molecules exhibits obvious difference relative to benzene (Fig. S3). Therefore, the substituents have affected the adsorption process to some extent, in agreement with the previous report.⁴

We shed light on how the electronegativity of the substituents has influenced the adsorption of the molecules on the SWCNs. The electron density of the benzene rings contained in the benzene derivatives could be altered by the substituents with different electronegativity, which affected the π - π interaction intensity between molecules and SWCNs.¹⁷ As we all know, the electron-withdrawing groups can bring about a lower electron density whereas electron-repelling groups can lead to a higher electron density. We found that as long as the electron density of the benzene ring of the molecules is reduced, in general, the corresponding experimental adsorption value is small, and the adsorption value is reversely large. Nevertheless, there are exceptions, i.e., a stronger electron density can not ensure a higher adsorption coefficient, and vice versa (Analysis of the electronegativity(substituent)-adsorption relationships can be seen in Text S1). This proves that the electron density changes of the benzene rings resulting from the substituents with different electronegativity seem not to be the only determinant factor for experimental adsorption values. Thus, we concluded two kinds of factors including π - π stacking and the substituent-SWCN interaction have affected

the adsorptions of the benzene derivatives on the SWCNs. The substituents, on the one hand, could alter the electron density of the benzene ring, thereby to indirectly influence the interactions with the SWCNs; on the other hand, they could directly interact with the SWCNs to influence the adsorptions.

5 However, the benzene-SWCN simulation results (Fig. S2) suggest that benzene prefers to interact with the SWCNs by a bridge configuration with a relatively lowest energy, consistent with the interaction configurations for the 25 molecules with the SWCNs.¹⁵ This proves that the substituents could not strikingly influence the π - π packing manner of benzene on the SWCNs. Or that is, relative to the π - π interaction, the substituents have a secondary effect on
10 the adsorption of the simple molecules on the SWCNs.

3.4 Electron rearrangement of the benzene derivatives

The benzene derivatives have experienced variations of conformation (surface characteristics, (Fig. 4), and dihedral angles (Φ) (Table S2) formed by four atoms (Fig. S4) and
15 quantum-chemical characteristics (dipole moment and orbital energies(Fig. 4))⁴⁸ at different levels due to the influence of SWCNs. Thus, this prompts us to consider a question of whether the electron density of the molecules has experienced the changes from a quantum-chemical point of view. To clarify this question, we compared the quantitative global total electrostatic potential (ESP) distribution on the surface of 13-IntMol and 13-Mol because this molecule
20 experienced a largest increase in the dipole moment. As shown in Fig. 5, the global minimums of the former and the latter are -42.348 kcal/mol and -37.029 kcal/mol, respectively, and the large negative value is owing to the lone pair of oxygen, implying an electron density reduction on the oxygen in methoxy. There is an increase of 0.821 kcal/mol in total ESP of -Cl in 13-IntMol relative to that of (-18.817 kcal/mol) 13-Mol. But the global maximum of total
25 ESP mainly arises from the positive charged C-H hydrogens of the benzene ring, with a value of 24.594 kcal/mol, which is obviously smaller than that of (26.698 kcal/mol) 13-IntMol. In conclusion, the property alternations of the simple molecules can be explained by the electron rearrangement resulted from the interference of the SWCNs.

We noticed that although dipole moments and various energies (Fig. S5 and Fig. S6) of the
30 SWCNs have been changed to some extent owing to the presence of the molecules, the order of magnitude of the energy differences of the SWCNs is significantly smaller than that of the molecules studied. This demonstrated the physical adsorptions of the molecules have very few effects on the SWCN's electronic structures, consistent with the conclusion of Woods et al.¹⁷ We speculated that large π - π systems in the SWCNs make them not easily affected by the
35 simple derivatives, and therefore only small changes in the CNTs' properties are expected.

3.5 Predicted energies vs. experimental adsorptions

We turned our attention to the relationship between various predicted energies ($E_{\text{Mol-SWCN}}^{\text{Mol-SWCN}}$, ΔE_{Ads} , ΔE_{Int} , $E_{\text{Def}}^{\text{Mol}}$ and $E_{\text{Def}}^{\text{SWCN}}$) and experimental adsorptions (Table S3). Although a largest correlation
40 coefficient (-0.370) (Table 3) between total energies ($E_{\text{Mol-SWCN}}^{\text{Mol-SWCN}}$) and experimental adsorptions is observed, the correlation is not significant. A highest $\Delta E_{\text{Ads}}-\Delta E_{\text{Int}}$ correlation of 0.884 (Sig.=0.01) (Table 3) displays ΔE_{Ads} is mainly governed by ΔE_{Int} , while $E_{\text{Def}}^{\text{Mol}}$ plays a relatively small impact on the adsorptions even though $E_{\text{Def}}^{\text{Mol}}$ can strikingly affect ΔE_{Ads} at the 0.05 level.

The energy-adsorption relationship above demonstrated that a less adsorption energy does not necessarily correspond to a higher experimental adsorption coefficient, and vice versa (Fig. 6). Hence, the predicted DFT energies do not show a strictly positive or negative correlation with experimental adsorptions. This motivates us to explore whether the local environment has influenced the molecule-SWCN interactions. The experimental adsorptions of the molecules studied were determined in water,²⁸ thus we optimized the molecule-SWCN conformation in water to explore the effects of the local environment on the adsorptions. The optimized results at the M062X/6-31G(d) levels indicate the final optimized conformations are basically agreement with the bridge manners of the molecules with the SWCNs in the gas phase (Fig. S7); moreover, there is no significant change in the correlations between experimental adsorptions and predicted energies (Table S4 and Table 3), and there are still two significant correlations, $\Delta E_{\text{Ads}} - \Delta E_{\text{Int}}$, and $\Delta E_{\text{Ads}} - E_{\text{Def}}^{\text{Mol}}$, which is same as those in the gas phase. This showed that solvent effects in water have not strikingly affected the π - π interaction manner between the molecules and the SWCN surfaces.

Although water molecules have weakly influenced the energy-adsorption relationship, their existence has still changed the CN's properties such as their dipole moments (Fig. 7) and conformational characteristics (Table S5), thereby to produce specific properties as being different from those in the gas phase. This also is supported by the report that the physical adsorptions of water molecules have significant effects on the electrical properties of the CN-based system.^{49, 50} According to the molecule-SWCN interaction modes, we speculated that on the one hand, the adsorption of water molecules on the SWCNs might disturb the interactions of the derivatives with the SWCNs; on the other hand, the interactions (for example, the formation of hydrogen bonding) between H₂O molecules and the benzene derivatives might influence the molecule-SWCN interactions. This can be further understood from the analysis that the variable, i.e., H-bond donor capacity, in the QSAR model has a significant effect on adsorption coefficients. Water molecules might change H-bond donor capacity of the derivatives, thus affecting molecular adsorptions on the SWCNs.

4. Conclusions

We employ QSAR modeling and DFT calculations to explore the adsorption characteristics of simple molecules on SWCNs. The QSAR model reveals a favorable predictive capability, and can be utilized to predict the molecule-SWCN adsorption. We report that π - π stacking dominates the adsorption of the simple benzene derivatives on the SWCNs, while the substituents play a secondary effect on the adsorption process. Our investigations also demonstrate although the molecules and the SWCNs can mutually affect their properties, the molecules have experienced a significant alternation of electronic structures relative to the SWCNs. In addition, these predicted energies do not show a significant positive or negative correlation with experimental adsorptions in both the gas phase and water.

One might modify functional groups of the molecules to acquire expected adsorption effects on the CNs, and further to carry out noncovalent functionalization of CNs, also utilize CNs to adsorb organic compounds from the surrounding environments. Although we explored the interaction mechanisms of the molecules with SWCNs instead of MWCNs, a molecular level understanding of the molecule-SWCN interactions provides valuable insights into the

structure-property relationship of nanotube-based materials which are important for nanomaterial, biomaterial, and environmental research.

Conflict of interest

5 The authors declare no conflict of interest.

Acknowledgments

G.L. is thankful for financial support from the National Natural Science Foundation of China (No.10901169), the Natural Science Foundation Project of Chongqing CSTC (No. cstc2012gg-gjhz10003), and the Fundamental Research Funds for the Central Universities (No. CQDXWL-2014-Z009). J.Z. thanks the National Science Foundation (CAREER Award CBET-0952624 and CBET-1158447) for financial support.

References

- 15 1 A. Oberlin, M. Endo and T. Koyama, Filamentous growth of carbon through benzene decomposition, *J. Cryst. Growth*, 1976, **32**, 335-349.
- 2 P. Avouris, Molecular electronics with carbon nanotubes, *Acc. Chem. Res.*, 2002, **35**, 1026-1034.
- 3 X. Q. Zhang, H. Li and K. M. Liew, The structures and electrical transport properties of germanium nanowires encapsulated in carbon nanotubes, *J. Appl. Phys.*, 2007, **102**, 073709.
- 20 4 K. Yang and B. Xing, Adsorption of organic compounds by carbon nanomaterials in aqueous phase: Polanyi theory and its application, *Chem. Rev.*, 2010, **110**, 5989-6008.
- 5 A. E. Nel, L. Madler, D. Velegol, T. Xia, E. M. Hoek, P. Somasundaran, F. Klaessig, V. Castranova and M. Thompson, Understanding biophysicochemical interactions at the nano-bio interface, *Nat Mater*, 2009, **8**, 543-557.
- 25 6 S. T. Kim, K. Saha, C. Kim and V. M. Rotello, The role of surface functionality in determining nanoparticle cytotoxicity, *Acc. Chem. Res.*, 2012, **46**, 681-691.
- 7 J. Lin, H. Zhang, Z. Chen and Y. Zheng, Penetration of lipid membranes by gold nanoparticles: insights into cellular uptake, cytotoxicity, and their relationship, *ACS Nano*, 2010, **4**, 5421-5429.
- 30 8 A. G. Kanaras, F. S. Kamounah, K. Schaumburg, C. J. Kiely and M. Brust, Thioalkylated tetraethylene glycol: a new ligand for water soluble monolayer protected gold clusters, *Chem. Commun. (Camb.)*, 2002, 2294-2295.
- 9 J. Chen, M. A. Hamon, H. Hu, Y. Chen, A. M. Rao, P. C. Eklund and R. C. Haddon, Solution properties of single-walled carbon nanotubes, *Science*, 1998, **282**, 95-98.
- 35 10 F. Wang, Y. C. Wang, S. Dou, M. H. Xiong, T. M. Sun and J. Wang, Doxorubicin-tethered responsive gold nanoparticles facilitate intracellular drug delivery for overcoming multidrug resistance in cancer cells, *ACS Nano*, 2011, **5**, 3679-3692.
- 11 A. Hirsch, Functionalization of single-walled carbon nanotubes, *Angew. Chem. Int. Ed. Engl.*, 2002, **41**, 1853-1859.
- 40 12 R. Demichelis, Y. Noël, P. D'Arco, M. Rérat, C. M. Zicovich-Wilson and R. Dovesi,

- Properties of Carbon Nanotubes: An ab Initio Study Using Large Gaussian Basis Sets and Various DFT Functionals, *J. Phys. Chem. C*, 2011, **115**, 8876-8885.
- 13 Y. Zhao and D. G. Truhlar, Density Functional Theory for Reaction Energies: Test of Meta and Hybrid Meta Functionals, Range-Separated Functionals, and Other High-Performance
5 Functionals, *J. Chem. Theory Comput.*, 2011, **7**, 669-676.
- 14 D. A. Britz and A. N. Khlobystov, Noncovalent interactions of molecules with single walled carbon nanotubes, *Chem. Soc. Rev.*, 2006, **35**, 637-659.
- 15 F. Tournus and J. C. Charlier, Ab initio study of benzene adsorption on carbon nanotubes, *Phys. Rev. B*, 2005, **71**, 165421.
- 10 16 E. S. Alldredge, S. C. Badescu, N. Bajwa, F. K. Perkins, E. S. Snow and T. L. Reinecke, Adsorption of nitro-substituted aromatics on single-walled carbon nanotubes, *Phys. Rev. B*, 2010, **82**, 125418.
- 17 L. M. Woods, Ş. C. Bădescu and T. L. Reinecke, Adsorption of simple benzene derivatives on carbon nanotubes, *Phys. Rev. B*, 2007, **75**, 155415.
- 15 18 O. G. Apul, Q. L. Wang, T. Shao, J. R. Rieck and T. Karanfil, Predictive Model Development for Adsorption of Aromatic Contaminants by Multi-Walled Carbon Nanotubes, *Environ. Sci. Technol.*, 2013, **47**, 2295-2303.
- 19 C. Hansch, P. P. Maloney, T. Fujita and R. M. Muir, Correlation of Biological Activity of Phenoxyacetic Acids with Hammett Substituent Constants and Partition Coefficients,
20 *Nature*, 1962, **194**, 178-180.
- 20 A. Cherkasov, E. N. Muratov, D. Fourches, A. Varnek, I. I. Baskin, M. Cronin, J. Dearden, P. Gramatica, Y. C. Martin, R. Todeschini, V. Consonni, V. E. Kuz'min, R. Cramer, R. Benigni, C. Yang, J. Rathman, L. Terfloth, J. Gasteiger, A. Richard and A. Tropsha, QSAR Modeling: Where Have You Been? Where Are You Going To?, *J. Med. Chem.*, 2014, **57**,
25 4977-5010.
- 21 G. Liang, L. Yang, Z. Chen, H. Mei, M. Shu and Z. Li, A set of new amino acid descriptors applied in prediction of MHC class I binding peptides, *Eur. J. Med. Chem.*, 2009, **44**, 1144-1154.
- 22 T. Puzyn, D. Leszczynska and J. Leszczynski, Toward the development of "nano-QSARs":
30 advances and challenges, *Small*, 2009, **5**, 2494-2509.
- 23 T. Puzyn, B. Rasulev, A. Gajewicz, X. Hu, T. P. Dasari, A. Michalkova, H. M. Hwang, A. Toropov, D. Leszczynska and J. Leszczynski, Using nano-QSAR to predict the cytotoxicity of metal oxide nanoparticles, *Nat Nanotechnol*, 2011, **6**, 175-178.
- 24 J. C. Ianni, V. Annamalai, P.-W. Phuan, M. Panda and M. C. Kozlowski, A Priori
35 Theoretical Prediction of Selectivity in Asymmetric Catalysis: Design of Chiral Catalysts by Using Quantum Molecular Interaction Fields, *Angew. Chem. Int. Ed.*, 2006, **45**, 5502-5505.
- 25 J. G. Cumming, A. M. Davis, S. Muresan, M. Haeberlein and H. Chen, Chemical predictive modelling to improve compound quality, *Nat. Rev. Drug Discov.*, 2013, **12**, 948-962.
- 40 26 D. Fourches, D. Pu, C. Tassa, R. Weissleder, S. Y. Shaw, R. J. Mumper and A. Tropsha, Quantitative nanostructure-activity relationship modeling, *ACS Nano*, 2010, **4**, 5703-5712.
- 27 X. R. Xia, N. A. Monteiro-Riviere, S. Mathur, X. Song, L. Xiao, S. J. Oldenberg, B. Fadeel and J. E. Riviere, Mapping the surface adsorption forces of nanomaterials in biological systems, *ACS Nano*, 2011, **5**, 9074-9081.

- 28 X. R. Xia, N. A. Monteiro-Riviere and J. E. Riviere, An index for characterization of nanomaterials in biological systems, *Nat Nanotechnol*, 2010, **5**, 671-675.
- 29 S. E. Wheeler and K. N. Houk, Substituent Effects in the Benzene Dimer are Due to Direct Interactions of the Substituents with the Unsubstituted Benzene, *J. Am. Chem. Soc.*, 2008, **130**, 10854-10855.
- 5 30 C. A. Hunter and J. K. M. Sanders, The nature of .pi.-.pi. interactions, *J. Am. Chem. Soc.*, 1990, **112**, 5525-5534.
- 31 C. F. Poole, S. K. Poole and M. H. Abraham, Recommendations for the determination of selectivity in micellar electrokinetic chromatography, *J. Chromatogr. A*, 1998, **798**, 207-222.
- 10 32 X. R. Xia, R. E. Baynes, N. A. Monteiro-Riviere and J. E. Riviere, A system coefficient approach for quantitative assessment of the solvent effects on membrane absorption from chemical mixtures, *SAR QSAR Environ. Res.*, 2007, **18**, 579-593.
- 33 B. Pan and B. Xing, Adsorption Mechanisms of Organic Chemicals on Carbon Nanotubes, *Environ. Sci. Technol.*, 2008, **42**, 9005-9013.
- 15 34 M. H. Abraham, H. S. Chadha, F. Martins, R. C. Mitchell, M. W. Bradbury and J. A. Gratton, Hydrogen bonding - Part 46: A review of the correlation and prediction of transport properties by an LFER method: physicochemical properties, brain penetration and skin permeability, *Pestic. Sci.*, 1999, **55**, 78-88.
- 20 35 Y. Zhao and D. Truhlar, The M06 suite of density functionals for main group thermochemistry, thermochemical kinetics, noncovalent interactions, excited states, and transition elements: two new functionals and systematic testing of four M06-class functionals and 12 other functionals, *Theor. Chem. Acc.*, 2008, **120**, 215-241.
- 36 M. Shahlaei, Descriptor selection methods in quantitative structure-activity relationship studies: a review study, *Chem. Rev.*, 2013, **113**, 8093-8103.
- 25 37 K. C. Chou and H. B. Shen, Recent progress in protein subcellular location prediction, *Anal. Biochem.*, 2007, **370**, 1-16.
- 38 P. Lazar, F. Karlicky, P. Jurecka, M. Kocman, E. Otyepkova, K. Safarova and M. Otyepka, Adsorption of Small Organic Molecules on Graphene, *J. Am. Chem. Soc.*, 2013, **135**, 6372-6377.
- 30 39 E. Cancès, B. Mennucci and J. Tomasi, A new integral equation formalism for the polarizable continuum model: Theoretical background and applications to isotropic and anisotropic dielectrics, *J. Chem. Phys.*, 1997, **107**, 3032-3041.
- 40 M. J. Frisch, G. W. Trucks, H. B. Schlegel, G. E. Scuseria, M. A. Robb, J. R. Cheeseman, G. Scalmani, V. Barone, B. Mennucci, G. A. Petersson, H. Nakatsuji, M. Caricato, X. Li, H. P. Hratchian, A. F. Izmaylov, J. Bloino, G. Zheng, J. L. Sonnenberg, M. Hada, M. Ehara, K. Toyota, R. Fukuda, J. Hasegawa, M. Ishida, T. Nakajima, Y. Honda, O. Kitao, H. Nakai, T. Vreven, J. A. Montgomery, Jr., J. E. Peralta, F. Ogliaro, M. Bearpark, J. J. Heyd, E. Brothers, K. N. Kudin, V. N. Staroverov, R. Kobayashi, J. Normand, K. Raghavachari, A. Rendell, J. C. Burant, S. S. Iyengar, J. Tomasi, M. Cossi, N. Rega, N. J. Millam, M. Klene, J. E. Knox, J. B. Cross, V. Bakken, C. Adamo, J. Jaramillo, R. Gomperts, R. E. Stratmann, O. Yazyev, A. J. Austin, R. Cammi, C. Pomelli, J. W. Ochterski, R. L. Martin, K. Morokuma, V. G. Zakrzewski, G. A. Voth, P. Salvador, J. J. Dannenberg, S. Dapprich, A. D. Daniels, Ö. Farkas, J. B. Foresman, J. V. Ortiz, J. Cioslowski and D. J. Fox, *Gaussian 09*, 2009, Gaussian, Inc.: Wallingford CT.

- 41 K. MH, N. CJ and N. J, , *Applied Linear Regression Models*, 2004, **4th edition**, McGraw-Hill Irwin.
- 42 P. Gramatica, Principles of QSAR models validation: internal and external, *QSAR Comb. Sci.*, 2007, **26**, 694-701.
- 5 43 G. Cruciani, P. Crivori, P. A. Carrupt and B. Testa, Molecular fields in quantitative structure-permeation relationships: the VolSurf approach, *J. Mol. Struct. THEOCHEM*, 2000, **503**, 17-30.
- 44 K. Yang, W. Wu, Q. Jing and L. Zhu, Aqueous Adsorption of Aniline, Phenol, and their Substitutes by Multi-Walled Carbon Nanotubes, *Environ. Sci. Technol.*, 2008, **42**, 7931-7936.
- 10 45 P. Wu, R. Chaudret, X. Hu and W. Yang, Noncovalent Interaction Analysis in Fluctuating Environments, *J. Chem. Theory Comput.*, 2013, **9**, 2226-2234.
- 46 E. R. Johnson, S. Keinan, P. Mori-Sánchez, J. Contreras-García, A. J. Cohen and W. Yang, Revealing Noncovalent Interactions, *J. Am. Chem. Soc.*, 2010, **132**, 6498-6506.
- 15 47 J. Zhao, J. P. Lu, J. Han and C.-K. Yang, Noncovalent functionalization of carbon nanotubes by aromatic organic molecules, *Appl. Phys. Lett.*, 2003, **82**, 3746-3748.
- 48 M. Karelson, V. S. Lobanov and A. R. Katritzky, Quantum-Chemical Descriptors in QSAR/QSPR Studies, *Chem. Rev.*, 1996, **96**, 1027-1044.
- 49 A. Zahab, L. Spina, P. Poncharal and C. Marliere, Water-vapor effect on the electrical conductivity of a single-walled carbon nanotube mat, *Phys. Rev. B*, 2000, **62**, 10000-10003.
- 20 50 W. Kim, A. Javey, O. Vermesh, O. Wang, Y. M. Li and H. J. Dai, Hysteresis caused by water molecules in carbon nanotube field-effect transistors, *Nano Lett.*, 2003, **3**, 193-198.
- 51 T. Lu and F. Chen, Multiwfn: A multifunctional wavefunction analyzer, *J. Comput. Chem.*, 2011, **33**, 580-592.

25

30

35

40

Table 1 Structures and adsorption coefficients of 25 simple molecules

No.	Name	Experimental $\log k$	Predicted $\log k$	
			Regression modeling	Cross-validation
1	chlorobenzene	3.25	3.33	3.38
2	ethylbenzene	3.19	3.24	3.26
3	p-xylene	3.26	3.25	3.25
4	propylbenzene	3.76	3.66	3.64
5	4-chlorotoluene	3.82	3.84	3.85
6	phenol	2.87	2.72	2.67
7	benzonitrile	3.04	3.13	3.30
8	4-fluorophenol	2.68	2.65	2.59
9	benzyl alcohol	2.10	2.11	2.12
10	iodobenzene	3.26	3.33	3.36
11	3-methylphenol	3.08	3.11	3.13
12	methyl benzoate	3.70	3.86	3.91
13	4-chloroanisole	4.07	4.06	4.06
14	phenethyl alcohol	2.54	2.56	2.57
15	3-methylbenzyl alcohol	2.85	2.88	2.90
16	4-ethylphenol	3.62	3.61	3.60
17	3,5-dimethylphenol	3.49	3.53	3.55
18	ethyl benzoate	4.14	3.97	3.93
19	methyl 2-methylbenzoate	4.12	4.04	4.01
20	naphthalene	4.44	4.27	4.24
21	3-chlorophenol	3.62	3.68	3.73
22	4-nitrotoluene	4.44	4.47	4.51
23	4-chloroacetophenone	4.28	4.17	4.09
24	1-methylnaphthalene	4.89	5.03	5.14
25	biphenyl	5.18	5.19	5.20

5

10

15

Table 2 Meaning, coefficients, statistical values of 8 variables in the MLR-based QSAR model

No.	Variable meaning	Coefficient	t-test value	Partial coefficient	Variance inflation factor
1	Capacity factor	0.387	6.598	0.855	7.011
2	Hydrophobic volume	0.311	6.086	0.836	5.627
3	Contact distance	0.095	3.647	0.674	1.352
4	H-bond donor capacity	-0.471	-9.951	-0.928	4.630
5	Hydrophilic integrity moment	0.117	2.305	0.499	5.130
6	Surface rugosity	0.482	10.745	0.937	4.336
7	Polar volume	0.079	2.320	0.502	2.339
8	Mass density	0.202	4.337	0.735	1.812
9	Constant	3.630	/	/	/

5

10

15

20

25

30

Table 3 Correlations between predicted energies and experimental adsorptions (*logk*) in the gas phase and water

	$E_{\text{Mol-SWCN}}^{\text{Mol-SWCN a}}$	$\Delta E_{\text{Ads}}^{\text{b}}$	$\Delta E_{\text{Int}}^{\text{c}}$	$E_{\text{Def}}^{\text{Mol d}}$	$E_{\text{Def}}^{\text{SWCN e}}$	<i>logk</i>
$E_{\text{Mol-SWCN}}^{\text{Mol-SWCN}}$	1.000					
ΔE_{Ads}	0.183/0.128 ^f	1.000				
ΔE_{Int}	0.105/0.168	0.884 ^{**} /0.590 ^{**g}	1.000			
$E_{\text{Def}}^{\text{Mol}}$	0.250/-0.042	0.490 [*] /0.622 ^{**}	0.079/-0.243	1.000		
$E_{\text{Def}}^{\text{SWCN}}$	-0.096/0.094	0.043/-0.118	-0.124/-0.381	-0.120/0.024	1.000	
<i>logk</i>	-0.370/-0.370	-0.254/-0.133	-0.318/-0.381	0.143/0.275	-0.193/-0.167	1.000

a: Total energy, b: Adsorption energy, c: Interaction energy, d: Deformation energy for the molecules, e: Deformation energy for the SWCNs, f: The number before and after the slash represent the coefficient in the gas phase and water, respectively. ^g: ^{**}The correlation is significant at the 0.01 level (2-tailed), ^{*} The correlation is significant at the 0.05 level (2-tailed).

5

10

15

20

25

30

35

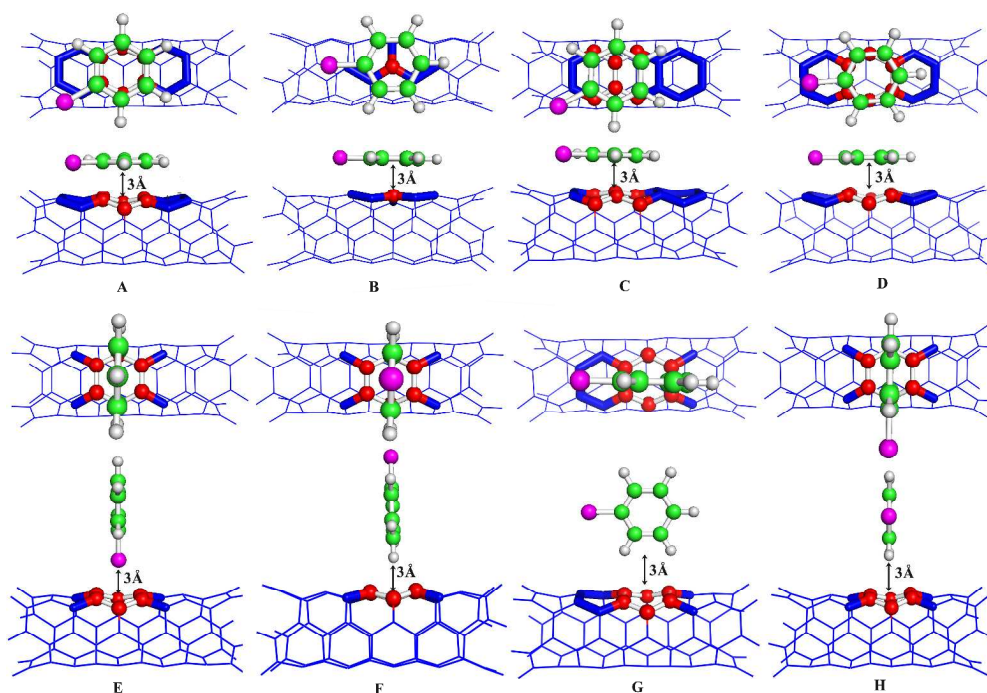


Fig. 1 Eight representative configurations for chlorobenzene-SWCN systems. Four parallel modes: (A) The hollow mode; (B) The umbrella mode; (C) The bridge mode; (D) The cross mode. Four perpendicular modes: (E) The R-pointing mode; (F) The para-R-pointing mode; (G and H) The two side-lying modes.

5

10

15

20

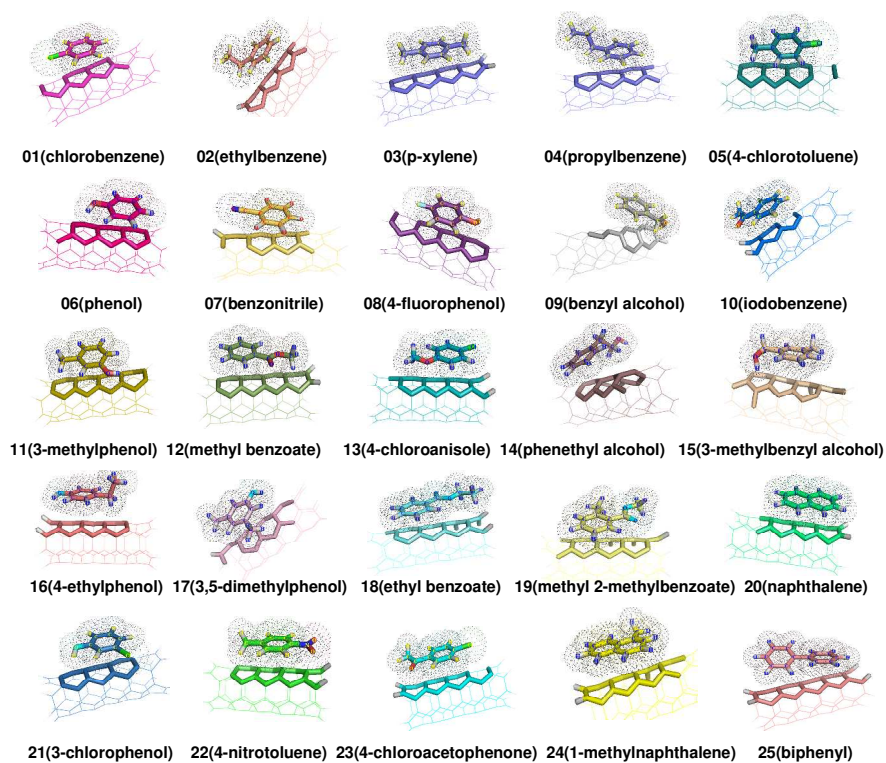


Fig. 2 The final optimized configurations of 25 molecule-SWCN systems in the gas phase. All the atoms of small molecules and their nearby carbon atoms of the SWCNs are highlighted to facilitate the observation of the interaction sites.

5

10

15

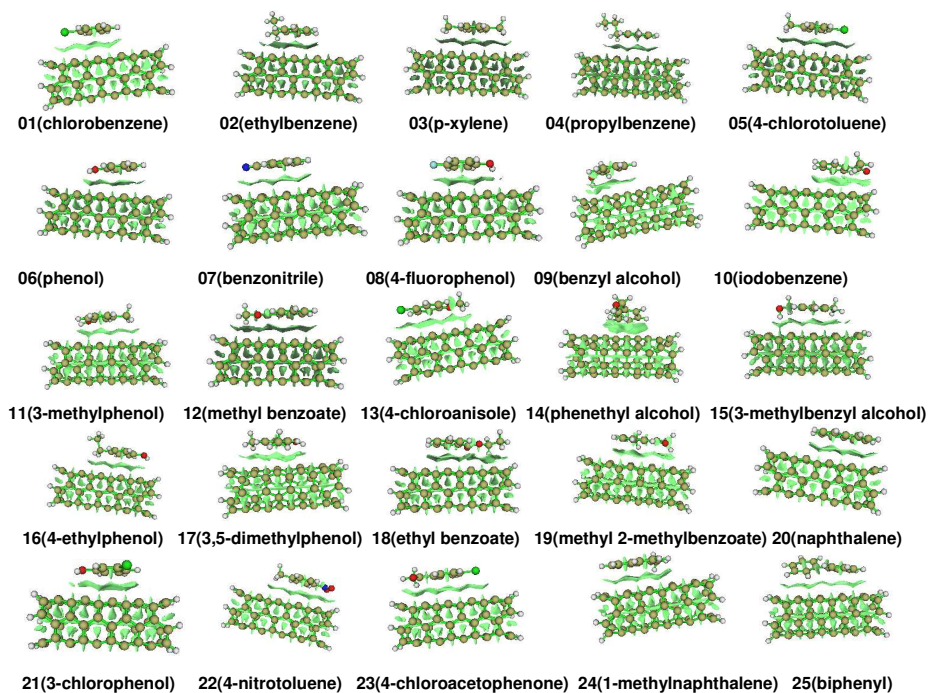


Fig. 3 The noncovalent and covalent effect visualization of 25 molecule-SWCN systems. The green clumps between molecules and SWCNs represent noncovalent interactions, and the green clumps within the molecules and the SWCNs represent covalent interactions.

5

10

15

20

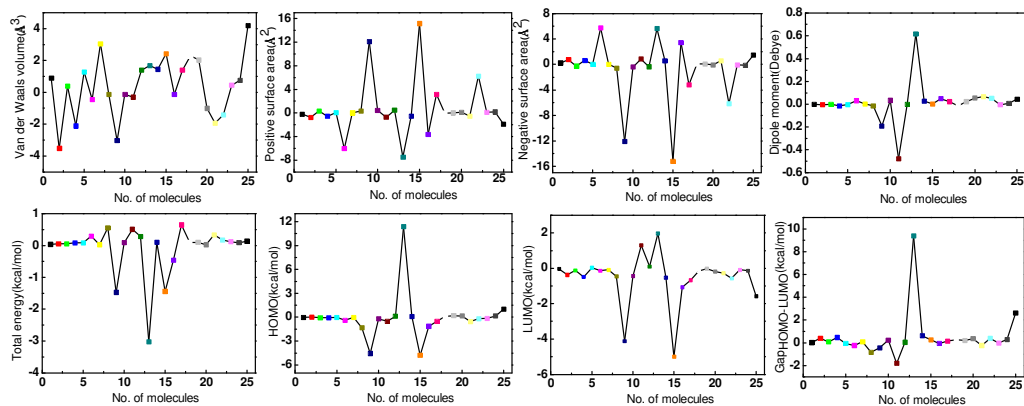


Fig. 4 The difference of surface characteristics, dipole moments and various energies between X-Mols and X-IntMols.

5

10

15

20

25

30

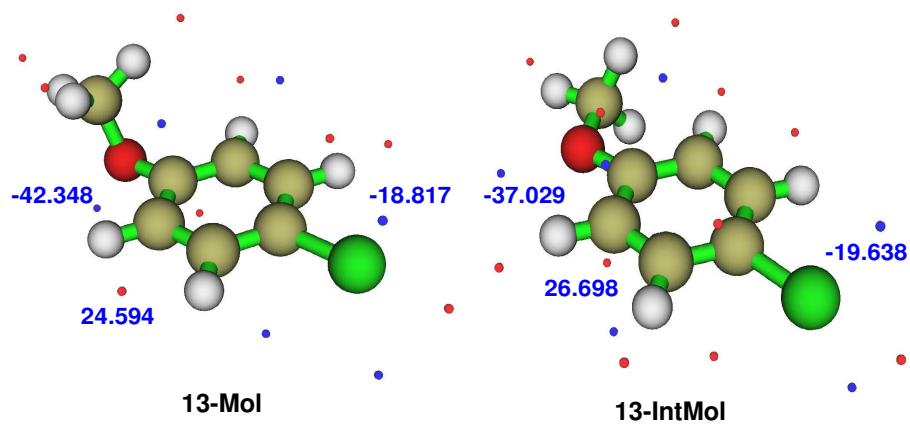


Fig. 5 The total electrostatic potential (kcal/mol) distribution of 13-Mol and 13-IntMol (4-chloroanisole). This figure is drawn using the Multiwfn software⁵¹.

5

10

15

20

25

30

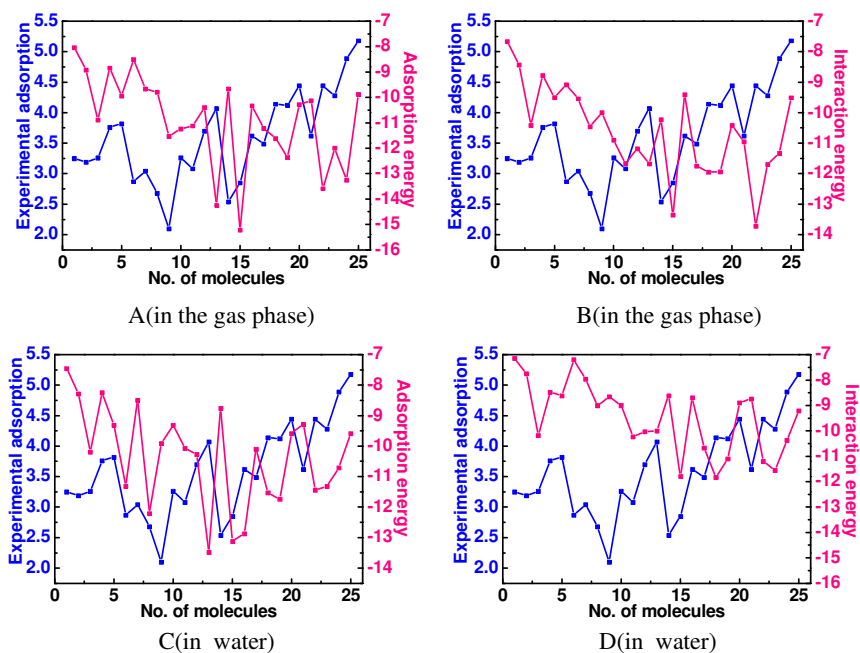


Fig. 6 The relationship between interaction energy (kcal/mol), adsorption energy (kcal/mol) and experimental adsorption ($\log k$) in the gas phase and water.

5

10

15

20

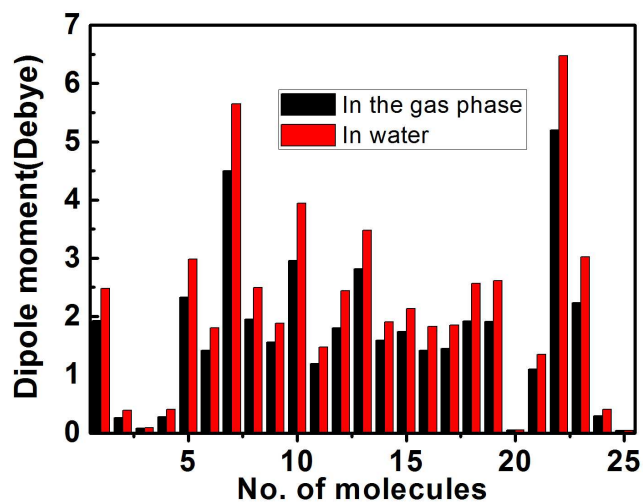


Fig. 7 The difference of dipole moment of 25 X-IntMols in the gas phase and water. The 25 molecules in water have relatively larger dipole moments than in the gas phase, showing that molecular polarities in water have strikingly been affected by water molecules.

5

10

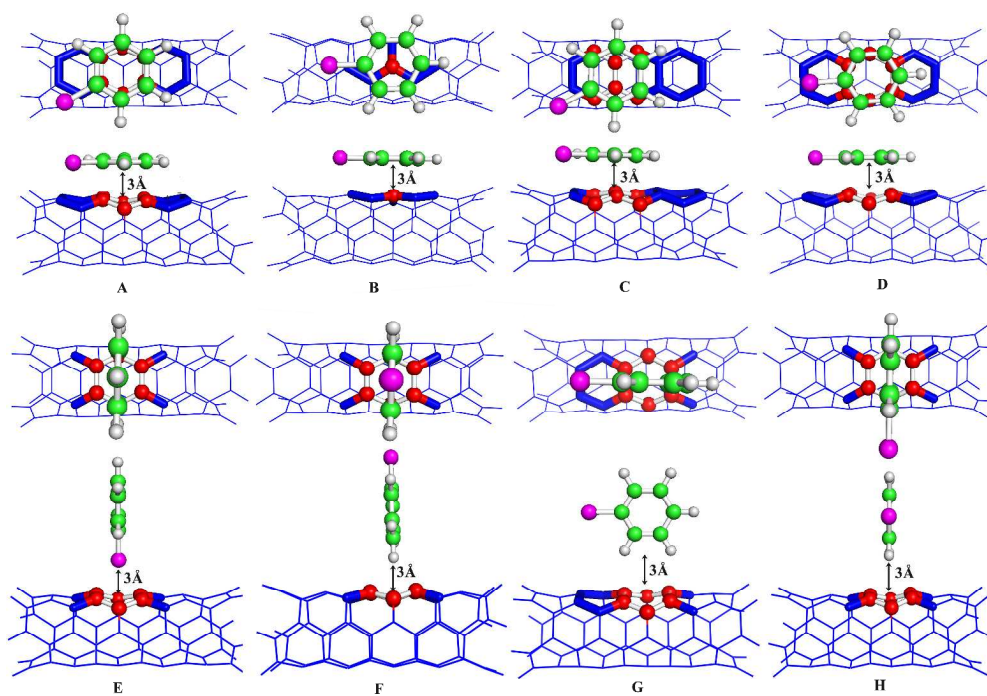
15

20

25

30

Table of contents



This work characterizes the adsorption characteristics of simple benzene derivatives on carbon nanotubes.

5